Journal of Renewable Materials
DOI:10.32604/jrm.2020.04399
Article

Tech Science Press

Influence of the Molecular Weight on PVA/GO Composite Membranes for Fuel Cell Applications

C. González-Guisasola[1], O. Gil-Castell[1,2], R. Teruel-Juanes[1] and A. Ribes-Greus[1,*]

[1]Instituto de Tecnología de Materiales (ITM), Universitat Politècnica de València, Valencia, 46022, Spain
[2]Departament d'Enginyeria Química, Universitat de València, Burjassot, 46100, Spain
*Corresponding Author: A. Ribes-Greus. Email: aribes@ter.upv.es
Received: 24 September 2018; Accepted: 28 March 2019

Abstract: Composite polymer electrolyte membranes were prepared with poly (vinyl alcohol) (PVA). Two different molecular weight (M_w), $67{\cdot}10^3$ and $130{\cdot}10^3$ g·mol^{-1} were selected, cross-linked with sulfosuccinic acid (SSA) and doped graphene oxide (GO). The effects on the membranes obtained from these polymers were characterized in order to evaluate the fuel cell performance. Electron microscopy showed a proper nanoparticle distribution in the polymer matrix. The chemical structure was evaluated by Fourier transform infrared spectroscopy. The absence of a crystalline structure and the enhancement on the thermal stability with the addition of 1% of GO was demonstrated by thermal characterization. Total transference number and protonic conductivity were correlated to the performance of a hydrogen fuel cell. Overall, a power increase in the composite membranes with lower molecular weight was observed. Shorter polymer chains may improve protonic conductivity and consequently the fuel cell performance.

Keywords: Fuel cell; graphene oxide; polarization; poly(vinyl alcohol); polyelectrolyte

1 Introduction

The proton exchange membrane fuel cells (PEMFC) are a potentially suitable renewable method to generate electrical power. For a long time, perfluorosulfonated (PFSA) membranes like Nafion® have been successfully used as polymeric material in these applications. However, this kind of material faces problems like intrinsic high costs and poor protonic conductivity in low humidity conditions [1]. Different approaches have been studied to avoid these problems. Most of them rely on the new combination of polymers and appropriate additives, as in the case of poly(vinyl alcohol) (PVA) membranes with inorganic or organic particles [2].

However, as PVA is non-proton conducting and water soluble it is usually submitted to a cross-linking process with sulfosuccinic acid (SSA), which not only improves its resistance to water but also its protonic conductivity, given the presence of proton conducting functional groups.

Although there are studies reporting the influence of the molecular weight (M_w) in fuel cells performance for perfluorosulfonated (PFSA) membranes [1] and polybenzimidazole (PBI) membranes [3]; there is limited information related to the effect of the molecular weight of composite PVA-based membranes containing GO.

In the present work, a systematic characterization with several ex-situ methods in terms of membrane morphology, chemical composition, thermal stability, total transference number, and protonic conductivity was applied to the prepared membranes, which were obtained with two different molecular weights of PVA and a constant 1% percentage of GO. These results were correlated with the finally behavior of these membranes as electrode assembly membrane (MEAs). The effect of the molecular weight of PVA were tested in a H_2/O_2 PEM monocell, which allowed determining the most favorable molecular weight in the design of new electrolytes.

2 Materials and Methods

2.1 Preparation of the Membranes

The GO nanoparticles were prepared by the Modified Hummers Method (MHM) from natural graphite (<20 μm) as described elsewhere [4–6]. First, a cold mixture of H_2SO_4, graphite and $NaNO_3$ was prepared. After 15 min, $KMnO_4$ was slowly added while stirring. Once the reaction took place, residual reagents were reduced by the addition of H_2O_2. The solid phase was separated and washed with diluted HCl and EtOH until neutral pH was reached. A series of PVA membranes with two different molecular weights: $67{\cdot}10^3$ g·mol^{-1} (86.7–88.7% hydrolyzed, Mowiol® 8-88) and $130{\cdot}10^3$ g·mol^{-1} (+99% hydrolyzed, Sigma Aldrich) were prepared by the solvent casting method [7]. The polymer granules were dissolved in distilled water, refluxed at 90°C and cold down. A 30 $\%wt_{PVA}$ SSA solution (Sigma-Aldrich) was then added. As functionalizing agent, a 1% suspension of sonicated GO was added to the mixture and casted in a circular mold at ambient temperature. Once dry, the membranes were cross-linked at 110°C for 2 h. These membranes, with a thickness of about 100–200 μm, were identified as 67kPVA/SSA, 67kPVA/SSA/GO, 130kPVA/SSA, 130kPVA/SSA/GO, respectively.

To test the membranes in a H_2/O_2 PEM monocell, the membranes were pre-conditioned submerging them in three baths of 3% H_2O_2, 0.5M H_2SO_4 and distilled water, respectively [8].

2.2 Membrane Characterisation

The surface morphology of the membrane and nanoparticle dispersion were investigated by means of a JEM 1010 transmission electron microscope (TEM).

The prepared membranes were examined by Fourier transform infrared (FTIR) spectroscopy in a Thermo Nicolet 5700 setup in the attenuated total reflectance mode. Air was employed as a background reference.

The thermal analysis of the membranes was performed using both differential scanning calorimetry (Mettler Toledo DSC 822) and thermogravimetry (Mettler Toledo TGA851). The DSC measurements were carried out from 25–220°C, under nitrogen atmosphere (50 ml·min^{-1}). Samples of about 3–4 mg were loaded into aluminum pans, and then heated to the desired temperature with a heating rate of 10°C ·min^{-1}. A second heating curve was also evaluated. A vacant aluminum pan was used as a reference during the whole experiment. The TGA data was recorded from 25 to 800°C, with a heating rate of 10°C ·min^{-1} and an oxidative atmosphere of O_2 at 50 ml·min^{-1}. The samples with a mass around 4 mg were introduced in 70 μL alumina crucibles. Moisture content was determined from the mass variation and peak temperature (T_p) in the first differential TG curve.

The direct current polarization curves were determined by using a lab-made controlled contact cell with a Keithley Femtoelectrometer 6420, in the working fuel cell temperature range from 30 to 120°C. Isothermal conditions were achieved placing the fixture inside a convection oven Heraeus UT 6.

The proton conductivity of the membranes was measured using an AC impedance method with a Concept 40 High Performance Dielectric Spectrometer (Novocontrol GmbH) in the frequency range from 10^{-2} to 10^7 Hz and room temperature. The proton conductivity was calculated using the Eq. (1).

$$\sigma = \frac{L}{R \cdot S} \tag{1}$$

The samples, previously soaked for 24 h in deionized water, were placed between two 20 mm stainless steel circular electrodes (SSE).

Fuel cell performance was tested by measuring the polarization curves of a cell. The membrane electrode assembly (MEA) was prepared by placing a hydrated 5 × 5 cm membrane between two carbon gas diffusion layers with Pt black powder on one side. Reactant gasses were obtained by electrolysis at room temperature and directly fed to the monocell. After galvanostatic activation, the I-V measurement of the single cell was recorded in an H-Tec fuel cell kit with a Keithley 2410 and a Fluke 73 DMM.

3 Results and Discussion

3.1 Structural Characterization

The achievement of suitable conductivity relies on the uniform and homogeneous dispersion of the GO nanoparticles. In this sense, the Fig. 1 shows the electronic micrographs of the membrane surfaces. The image of the 130kPVA/SSA/GO membrane displayed a smooth surface whereas in the 67kPVA/SSA/GO a particle clustering effect was noticed. It is known that GO suspensions may coagulate due to interaction between the charged groups on its surface and edges [9]. A higher molecular weight may have promoted a better interfacial adhesion and improved compatibility between the GO particles and PVA matrix.

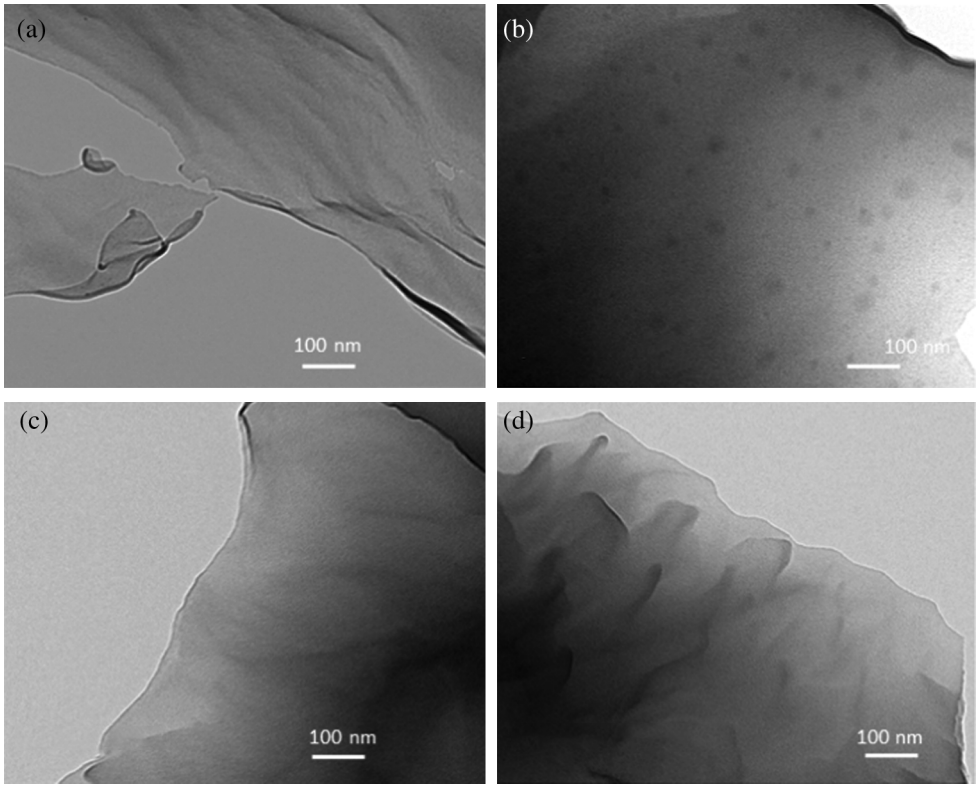

Figure 1: Surface micrographs of a) 67kPVA/SSA, b) 67kPVA/SSA/GO, c) 130kPVA/SSA and d) 130kPVA/SSA/GO

As well, the evaluation of the chemical structure of the composites may bring valuable information for an adequate application of the proposed composites. The infrared spectra of the PVA, SSA and GO are plotted in Fig. 2. For pure PVA, the broad band at 3597 cm^{-1} is assigned to the stretching vibration of hydroxyl groups [10]. At 2925 and at 2853 cm^{-1} the band corresponding to CH asymmetric stretching and CH symmetric stretching vibration was observed. The band 1732 cm^{-1} corresponded to the C=O stretching vibration and the peak at 1089 cm^{-1} indicated the C–O stretching of the PVA molecules.

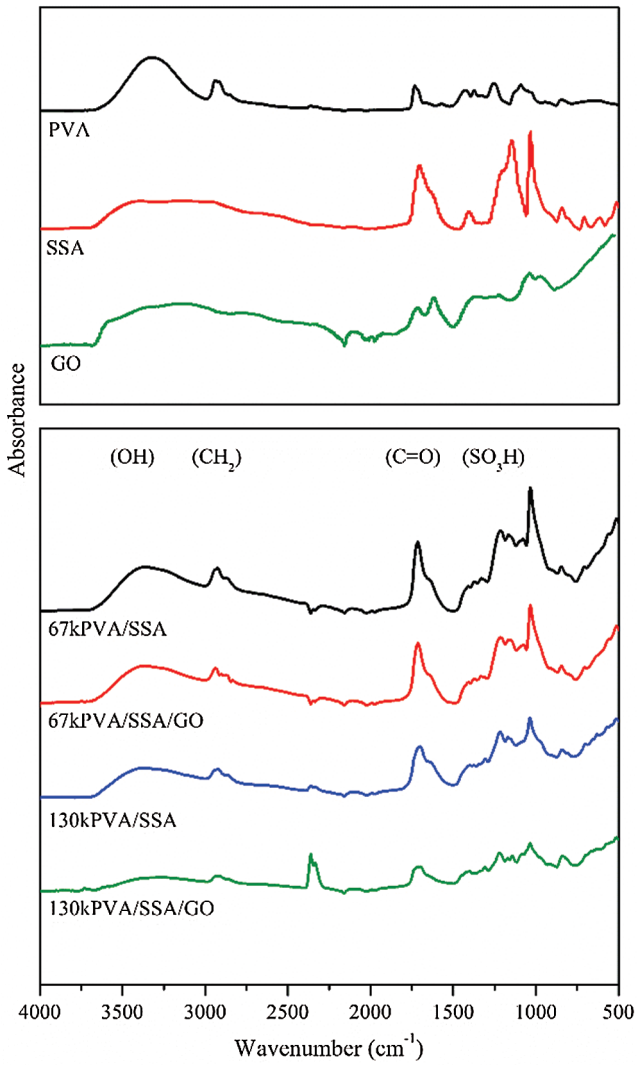

Figure 2: FTIR spectra of PVA, SSA, GO, 67kPVA/SSA, 67kPVA/SSA/GO, 130kPVA/SSA and 130kPVA/SSA/GO

The SSA spectrum showed several bands in the 3000–3600 cm^{-1} region related to water and the carboxyl groups (–COOH). The peak at 1031 cm^{-1} indicated the presence of $–SO_3H$ groups.

In the GO spectrum, a strong and broad absorption band between 3500 and 2500 cm^{-1} due to the –OH stretching vibration was observed. The bands at 1701 and 1036 cm^{-1} were associated to double and single bonds in the acid groups [11]. The peak at 1618 may be from skeletal vibrations of unoxidized graphitic domains and the adsorbed water molecules.

Fig. 2 shows the FTIR spectra of the membranes, where a stretching vibration band at 2900–3000 cm^{-1} associated to the CH/CH_2 was observed. The –OH stretching absorption band between 3000 and 3500 cm^{-1} indicated the existence of a strong intra and inter molecular hydrogen bonding [2]. The decrease in intensity and increase in width of the –OH band suggested a strong interaction due to the presence of SSA. The absorption peak between 1699 and 1714 cm^{-1}, corresponded to the stretching vibration of –C=O ester groups. The absorption peak at 1033–1035 cm^{-1} confirmed the presence of a sulfonic acid group. The increasing of PVA molecular weight does not induce remarkable differences in the spectrum.

3.2 Thermal Properties

The DSC thermograms of all composite membranes are shown in Fig. 3. These plots exhibited a rapid downward shift indicating a fast endothermic process above 100°C, which can be associated to the expulsion of water or the start of the decomposition of the membrane. The step change associated with the T_g was either too small or disappeared in the second heating to be established in Fig. 3 [12]. Similar effects have been observed in $PVA/H_3PO_4/H_2O$ systems [13]. The disappearance of the T_g indicated a good PVA/SSA cross-linking and good blending PVA/SSA with the GO particles. Differences in the PVA molecular weight does not produce significant changes in the thermograms.

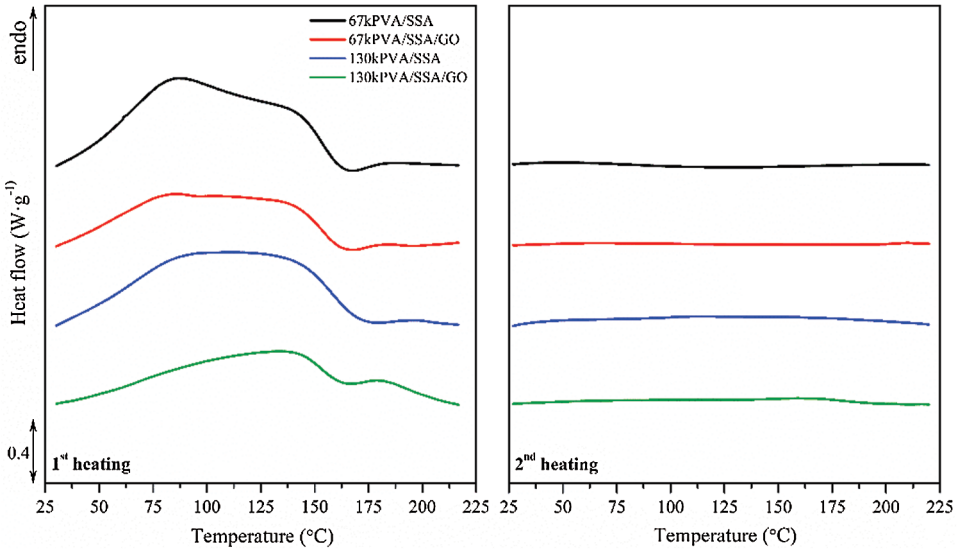

Figure 3: DSC thermograms of the first heating (left), and second heating (right) scans

3.3 Thermo-Oxidative Stability

In Fig. 4 the thermogravimetric analysis spectra of thermally cross-linked PVA/SSA with different GO contents is shown. The weight losses in the first (80–150°C), second (200–330°C) and third (400–450°C) stages can be attributed to the expulsion of water molecules from the polymer matrix or the decomposition of the alcohol group, the decomposition of sulfonic acid groups and the separation of the main chain of PVA followed by the decomposition of the polymer backbone happening above 450°C, respectively. Although no significant change in the thermogravimetric thermograms was observed initially, a small delay was recorded on the onset of the decomposition temperature for the membranes with lower molecular weight functionalized with GO. This implies that GO reduces the humidity loss because the oxygen rich groups of its surface establish hydrogen bonds with the alcohol groups of the polymer matrix and increases the thermal stability of the composites.

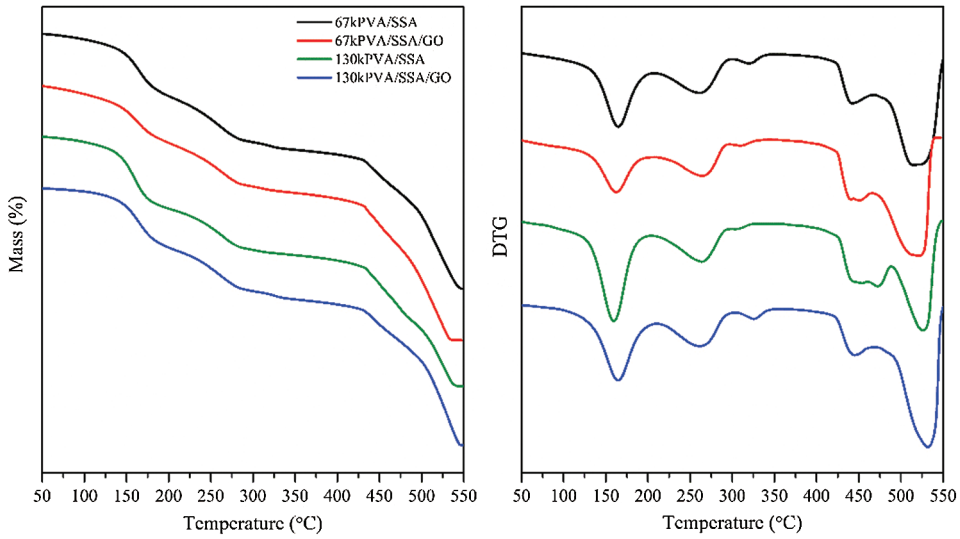

Figure 4: Thermo-oxidative stability in terms of thermogravimetric (left), and derivative thermogravimetric (DTG) (right) profiles

3.4 Polarization Current

The electronic conductivity, the ionic transference number and the protonic conductivity are properties that determine the behavior of the polymer electrolytes. Fig. 5 shows the polarization current curves over a range of positive temperatures. The electronic contribution to the total current is very low, which is essential for fuel cells membranes.

As non-selective parameter, the total ionic transference number was calculated according to the Eq. (2).

$$t_{ion} = \frac{(I_0 - I_{inf})}{I_0} \tag{2}$$

From the starting temperature to about 60°C, the values increased or changed very little. At higher temperatures the value started to decrease. This behavior was not observed in the membrane 130kPVA/SSA/GO, as the t_{ion} increased continuously with temperature. These results agree with the thermal analysis and indicate that longer polymer chains may interfere in the ionic paths of ions.

Fig. 6 shows the impedance (Z) and phase angle (Φ) of all the composite membranes at room temperature and the protonic conductivity (σ) is gathered in Tab. 1. It is noticeable that, under dry condition and in all cases, lower conductivity values were observed when GO was present. The proton conductivity of the nanocomposite membranes decreases with a load of filler, which could due to a blocking effect in the membranes. This means, the addition of too many planar nanoparticles obstructs the polymer chain movement in the proton cluster [14]. However, the proton conductivity values were higher in the membranes with lower molecular weight.

3.5 Fuel Cell Performance

Fig. 7 displays the potential and power curves for the membranes electrode assembly (MEAs) prepared in standard conditions. The curve corresponding to a Nafion®117 membrane was also included for comparison purposes. The open circuit voltage (OCV) for the 67kPVA/SSA/GO membranes (937 mV) are higher, compared to that of 130kPVA/SSA/GO membranes (662 mV) and consequently the maximum

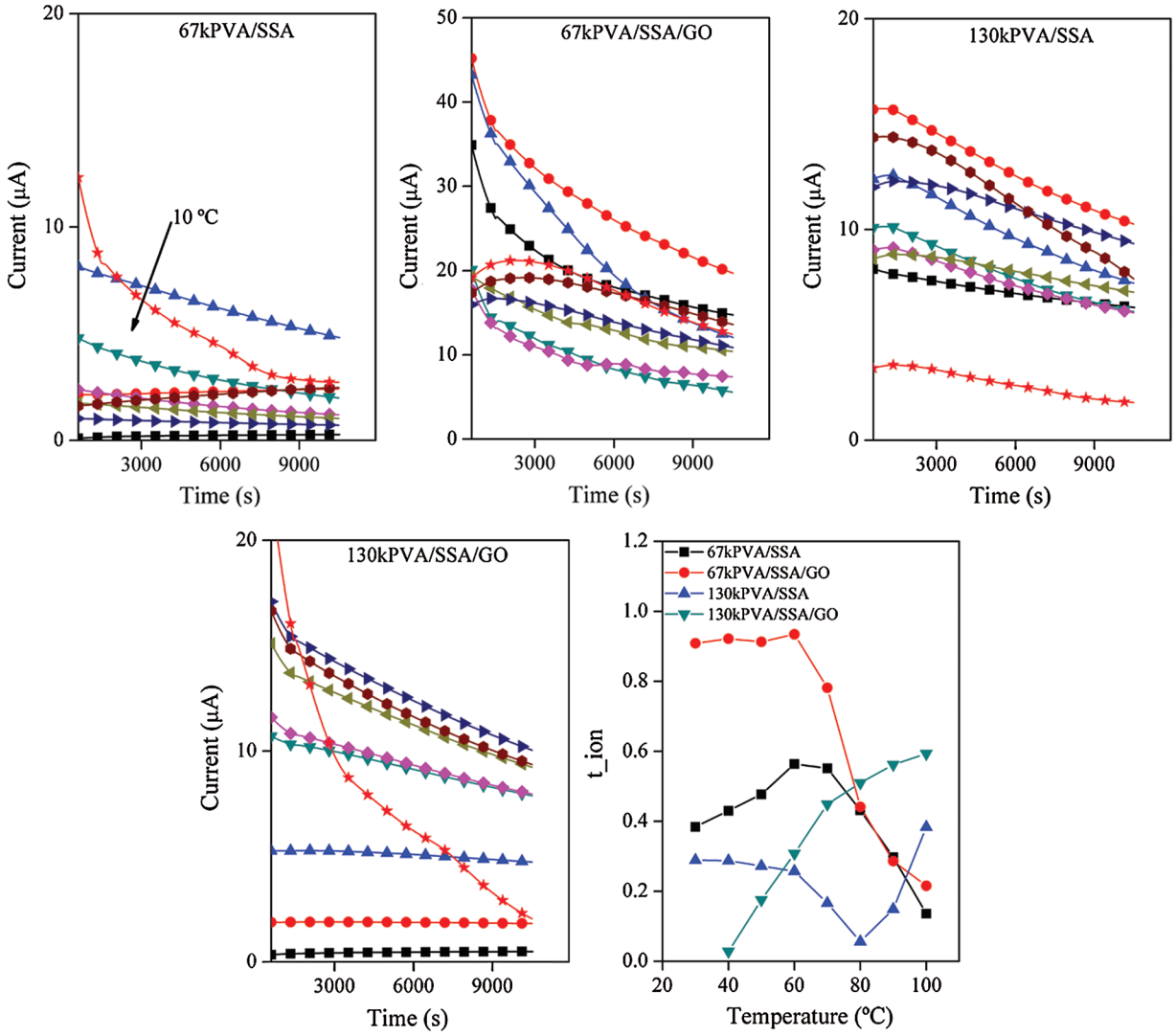

Figure 5: Polarization current and total ionic transference number for the composite membranes

power density of the 67kPVA/SSA/GO membranes are also higher than the 130kPVA/SSA/GO. These results are consistent with the higher ohmic resistance of the membrane.

The P-I curves were fitted according to the Eq. (3) and results are gathered in Tab. 1. It seems that shorter polymer chains may give a more compact cross-linked structure and closer functional groups, which in turn improve fuel cell performance. Results are similar to obtained with the commercial perfluorosulfonated membrane.

$$V = OCV - A \cdot \log\left(\frac{i}{i_0}\right) - R \cdot i \tag{3}$$

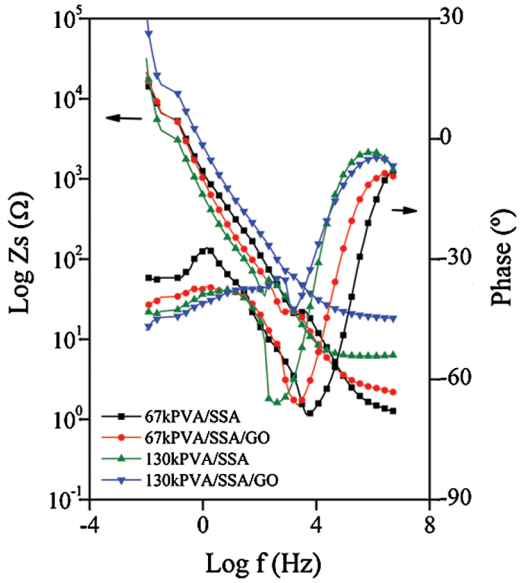

Figure 6: V *vs*. I and P *vs*. I curves for Nafion® and composite membranes, 293 K, pure H_2 and O_2

Table 1: Comparison of proton conductivity and fitting parameters for the prepared membranes

Membrane	Width (μm)	σ (mS·cm^{-1})	OCV (mV)	MPP (mW·cm^{-2})
67kPVA/SSA	127.9	2.06	937	7.07
67kPVA/SSA/GO	142.8	1.53	808	7.23
130kPVA/SSA	175.8	0.93	662	2.72
130kPVA/SSA/GO	102.8	0.17	830	4.94
Membrane	A (mV·dec^{-1})	i_0 (mA·cm^2)	R (mΩ)	R^2 (%)
67kPVA/SSA	52.00	0.16	17.00	97.3
67kPVA/SSA/GO	–	1.36	21.73	94.4
130kPVA/SSA	11.04	0.04	33.31	99.9
130kPVA/SSA/GO	33.80	0.05	18.05	99.9

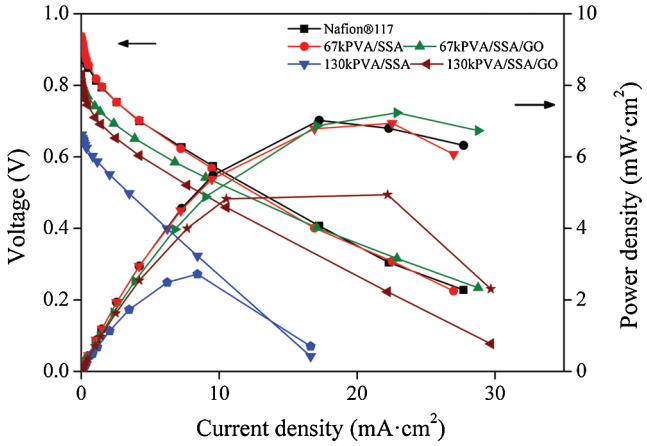

Figure 7: V *vs*. I and P *vs*. I curves for Nafion® and composite membranes, 293 K, pure H_2 and O_2

4 Conclusions

Composite polymer electrolyte membranes were successfully prepared with poly(vinyl alcohol) with two different molecular weights, cross-linked with sulfosuccinic acid and functionalized with graphene oxide. It was found that the addition of small percentages of GO increased the thermal stability by reducing the water content. The total ionic transfer number was higher in the membranes with lower molecular weight.

The potential and power curves, which define the fuel cell performance, reveal that the lower molecular weight PVA membranes (67kPVA/SSA/GO) have a similar behavior to the corresponding perfluorosulfonated membranes. Thus, the 67kPVA/SSA/GO electrolytes prepared with PVA, SSA and GO could be a feasible alternative, with lower cost and more respectful with the environment to the commercial membranes.

Acknowledgement: The authors would like to thank to support of the Spanish Ministry of Economy, Industry and Competitiveness, through the research project POLYDECARBOCELL (ENE2017-86711-C3-1-R) and to the Spanish Ministry of Education, Culture and Sports for the FPU grant for O. Gil-Castell (FPU13/01916).

Funding Statement: This study was funded by the Spanish Ministry of Economy, Industry and Competitiveness, through the research project POLYDECARBOCELL (ENE2017-86711-C3-1-R) and by the Spanish Ministry of Education, Culture and Sports through the FPU grant for O. Gil-Castell (FPU13/01916).

Conflicts of Interest: The authors declare that they have no conflicts of interest to report regarding the present study.

References

1. Peighambardoust, S. J., Rowshanzamir, S., Amjadi, M. (2010). Review of the proton exchange membranes for fuel cell applications. *International Journal of Hydrogen Energy, 35(17),* 9349–9384. DOI 10.1016/j.ijhydene.2010.05.017.
2. Gahlot, S., Sharma, P. P., Kulshrestha, V., Jha, P. K. (2014). SGO/SPES-based highly conducting polymer electrolyte membranes for fuel cell application. *ACS Applied Materials & Interfaces, 6(8),* 5595–5601. DOI 10.1021/am5000504.
3. Ossiander, T., Perchthaler, M., Heinzl, C., Schönberger, F., Völk, P. et al. (2016). Influence of membrane type and molecular weight distribution on the degradation of PBI-based HTPEM fuel cells. *Journal of Membrane Science, 509,* 27–35. DOI 10.1016/j.memsci.2016.02.037.
4. Hummers, W. S., Offeman, R. E. (1958). Preparation of graphitic oxide. *Journal of the American Chemical Society, 80(6),* 1339. DOI 10.1021/ja01539a017.
5. Shahriary, L., Athawale, A. (2014). Graphene oxide synthesized by using modified hummers approach. *International Journal of Renewable Energy and Environmental Engineering, 2(1),* 58–63.
6. González-Guisasola, C., Ribes-Greus, A. (2018). Dielectric relaxations and conductivity of cross-linked PVA/SSA/GO composite membranes for fuel cells. *Polymer Testing, 67,* 55–67. DOI 10.1016/j.polymertesting.2018.01.024.
7. Bao, C., Guo, Y., Song, L., Hu, Y. (2011). Poly(vinyl alcohol) nanocomposites based on graphene and graphite oxide: a comparative investigation of property and mechanism. *Journal of Materials Chemistry, 21(36),* 13942. DOI 10.1039/c1jm11662b.
8. Zawodzinski, T. A. (1993). Water uptake by and transport through nafion® 117 Membranes. *Journal of the Electrochemical Society, 140(4),* 1041. DOI 10.1149/1.2056194.
9. Liang, B. J., Huang, Y., Zhang, L., Wang, Y., Ma, Y. et al. (2009). Molecular-level dispersion of graphene into poly (vinyl alcohol) and effective reinforcement of their nanocomposites. *Advanced Functional Materials, 19(14),* 2297–2302. DOI 10.1002/adfm.200801776.

10. Socrates, G. (2004). *Infrared and raman characteristic groups frequencies: tables and charts*. West Sussex. John Wiley & Sons.
11. Gu, H., Yu, Y., Liu, X., Ni, B., Zhou, T. et al. (2012). Layer-by-layer self-assembly of functionalized graphene nanoplates for glucose sensing *in vivo* integrated with on-line microdialysis system. *Biosensors and Bioelectronics, 32(1),* 118–126. DOI 10.1016/j.bios.2011.11.044.
12. Vargas, M., Vargas, R., Mellander, B. E. (2000). More studies on the PVAl + H_3PO_2 + H_2O proton conductor gels. *Electrochimica Acta, 45(8–9),* 1399–1403. DOI 10.1016/S0013-4686(99)00350-3.
13. Fernández, M. E., Murillo, G., Vargas, R. A., Peña Lara, D., Diosa, J. E. (2017). Improvement of proton-exchange membranes based on (1–x) (H_3PO_2/PVA)-xTiO_2, *Ingeniería y Ciencia, 13(25),* 153–166.
14. Heo, Y., Im, H., Kim, J. (2013). The effect of sulfonated graphene oxide on Sulfonated Poly (Ether Ether Ketone) membrane for direct methanol fuel cells. *Journal of Membrane Science, 425,* 11–22. DOI 10.1016/j.memsci.2012.09.019.